Advances in Carbohydrate Chemistry and Biochemistry

Volume 62

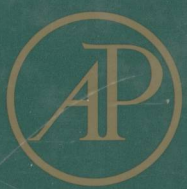

Advances in Carbohydrate Chemistry and Biochemistry

Editor
DEREK HORTON
The American University
Washington, DC

Volume 62

ELSEVIER

Amsterdam • Boston • Heidelberg • London • New York • Oxford
Paris • San Diego • San Francisco • Singapore • Sydney • Tokyo
Academic Press is an imprint of Elsevier

Academic Press is an imprint of Elsevier
Radarweg 29, PO BOX 211, 1000 AE Amsterdam, The Netherlands
Linacre House, Jordan Hill, Oxford OX2 8DP, UK
32 Jamestown Road, London NW1 7BY, UK
30 Corporate Drive, Suite 400, Burlington, MA 01803, USA
525 B Street, Suite 1900, San Diego, CA 92101-4495, USA

First edition 2009

ISBN: 978-0-12-374743-3
ISSN: 0065-2318

British Library Cataloguing in Publication Data
A catalogue record for this book is available from the British Library

Library of Congress Cataloging-in-Publication Data
A catalog record for this book is available from the Library of Congress

For information on all Academic Press publications visit our website at books.elsevier.com

Printed and bound in USA

09 10 10 9 8 7 6 5 4 3 2 1

Advances in
Carbohydrate Chemistry and Biochemistry

Volume 62

LIST OF CONTRIBUTORS

Rosalía Agusti, CHIDECAR, Departamento de Química Orgánica, Facultad de Ciencias Exactas y Naturales, Universidad de Buenos Aires, Pabellón II, Ciudad Universitaria, 1428 Buenos Aires, Argentina

Feng Cai, Department of Chemistry, Wayne State University, Detroit, MI 48202, USA

Bruce Coxon, National Institutes of Health, Bethesda, MD 20892, USA

David Crich, Department of Chemistry, Wayne State University, Detroit, MI 48202, USA

Alexei V. Demchenko, Department of Chemistry and Biochemistry, University of Missouri - St Louis, One University Boulevard, St Louis, MO 63121, USA

Robin Ferrier, Gracefield Research Central Sciences, Industrial Research Ltd., Lower Hutt, New Zealand

Rosa M. de Lederkremer, CHIDECAR, Departamento de Química Orgánica, Facultad de Ciencias Exactas y Naturales, Universidad de Buenos Aires, Pabellón II, Ciudad Universitaria, 1428 Buenos Aires, Argentina

Mario A. Monteiro, Department of Chemistry, University of Guelph, Guelph, ON N1G 2W1, Canada

Roberto Rizzo, Department of Life Sciences, University of Trieste, Via Licio Giorgieri, 34127 Trieste, Italy

James T. Smoot, Department of Chemistry and Biochemistry, University of Missouri - St Louis, One University Boulevard, St Louis, MO 63121, USA

Dennis M. Whitfield, Institute for Biological Sciences, National Research Council of Canada, 100 Sussex Drive, Ottawa, ON K1A 0R6, Canada

Baolin Wu, Department of Chemistry, Wayne State University, Detroit, MI 48202, USA

PREFACE

Sugars played a key role at the dawn of the nuclear magnetic resonance era. Foremost was Lemieux's demonstration that the magnitude of vicinal proton–proton spin couplings was related to the spatial orientation of the hydrogen atoms. Subsequently, Karplus presented an equation that quantifies the relationship between the NMR coupling constants of sugars and related molecules to the dihedral angle between the coupled nuclei. In this issue, Coxon (Bethesda, Maryland) provides a comprehensive survey of the many empirical variants of the Karplus-type equation that have been proposed over the years as NMR spectroscopy has evolved to become the indispensable key tool in carbohydrate characterization. The treatment covers spin couplings over three, four, and five bonds, and includes both protons and heteronuclei. The equations range from simple, two-parameter versions that depict only the torsional dependence of coupling constants, to complex 22-parameter forms that simulate the variation of the coupling with many different molecular properties. Earlier applications of NMR in the carbohydrate field were surveyed in this series by Hall in Volumes 19 and 29, by Coxon in Volume 27, and later by Csuk and Glänzer in Volume 46, and by Tvaroška and Taravel in Volume 51.

Three articles in this volume, written from different perspectives, focus on a central theme in carbohydrate science, namely the glycosidic linkage, its formation and cleavage. The presumed intermediates or transition states in these reactions have considerable oxacarbenium ion character. Using a computational approach, Whitfield (Ottawa) employs quantum mechanics to study the bonding characteristics of such ions, which are difficult to study experimentally. Focusing on the 2,3,4,6-tetra-*O*-methyl-D-galactopyranosyl cation and its 2-*O*-acetyl analogue, his treatment examines their detailed conformations (half-chair and skew) and calculated energies to demonstrate the potential of *in silico* methodology in understanding the reactivity of glycopyranosyl oxacarbenium ions.

Although glycoscientists have learned over the years how to isolate certain classes of naturally occurring complex carbohydrates, the availability of pure natural compounds remains inadequate to address many ongoing challenges. Chemical synthesis remains the essential resource for accessing complex oligosaccharides and glycoconjugates, to provide significant quantities of the pure natural structures as well as unnatural mimetics that are often of interest. In this volume, Smoot and Demchenko (St. Louis, Missouri) survey the drawbacks of traditional oligosaccharide syntheses that require extensive protecting-group manipulations between each glycosylation step, and discuss significant recent improvements that have emerged to circumvent the shortcomings of earlier approaches. Their article complements the classic chapter

in Volume 50 by Schmidt and Kinzy on the trichloroacetimidate methodology, the articles by Garegg in Volumes 52 and 59 focusing on thioglycoside procedures, and solid-state synthetic techniques as presented in Volume 58 by Plante, Palmacci, and Seeberger.

In a third related article, Cai, Wu, and Crich (Detroit, Michigan) focus on the particular situation in homoglycan synthesis where the glycon has an axial hydroxyl group at the 2-position. For the total synthesis of α-mannans and α-rhamnans the overall strategy involves construction of the 1,2-trans-axial glycosidic bond, whereas the β-mannans and β-rhamnans require additional steps post-glycosylation to generate the 1,2-*cis*-equatorial glycosidic linkage.

The glycobiology of *Trypanosoma cruzi*, the causative agent of Chagas' disease, has contributed significantly to the identification of target enzymes responsible for the construction of unique cell-surface molecules. Agusti and de Lederkremer (Buenos Aires) here discuss the structure of glycoinositolphospholipids in *T. cruzi*, both free and as protein anchors, that display unusual structural motifs, including galactofuranose, which are absent in mammals. The chemical synthesis of oligosaccharides containing Gal*f* is presented, as well as the use of the organism's trans-sialidase (TcTS) for synthetic purposes.

Many of the articles in earlier volumes of this *Advances* series remain of permanent reference value, but library holdings of the full series have not kept pace with growth of the carbohydrate field and the opening of many new research centers. In an important development, the publishers have now made full-text electronic access available, through *Science Direct,* to all previously published articles in every volume. Volume 1, which appeared in 1945 with the title *Advances in Carbohydrate Chemistry*, under the editorship of Ward Pigman and Melville L. Wolfrom, featured as its opening article a chapter on the classic Fischer cyanohydrin reaction for ascent of the sugar chain, authored by the great carbohydrate pioneer Claude S. Hudson. The series title was changed with Volume 24 to *Advances in Carbohydrate Chemistry and Biochemistry* to reflect the broadening impact of carbohydrates in the biological field.

Grateful thanks are expressed to three senior statesmen of the carbohydrate community, Laurens Anderson, Hans Baer, and John Brimacombe, who as members of the Board of Advisors have helped over the years to guide these *Advances* with their own contributions, their valuable insight, and their mentoring service to others providing significant articles to the series. With this issue, Robin Ferrier (New Zealand) and Mario Monteiro (Guelph, Ontario), the first and last doctoral students of the late Gerald Aspinall, pay tribute to the enormous contributions made by their mentor to the carbohydrate field, especially in the area of polysaccharide structural

methodology. Roberto Rizzo (Trieste) provides an account of the life and work of Vittorio Crescenzi, and his notable investigations on polysaccharide technology and the physicochemical behavior of biopolymers in solution.

A sad note is of the recent deaths of several great carbohydrate pioneers of the twentieth century, including Roger Jeanloz, Bengt Lindberg, and Per Garegg, whose work will be commemorated in a future volume.

DEREK HORTON

Washington, DC
November, 2008

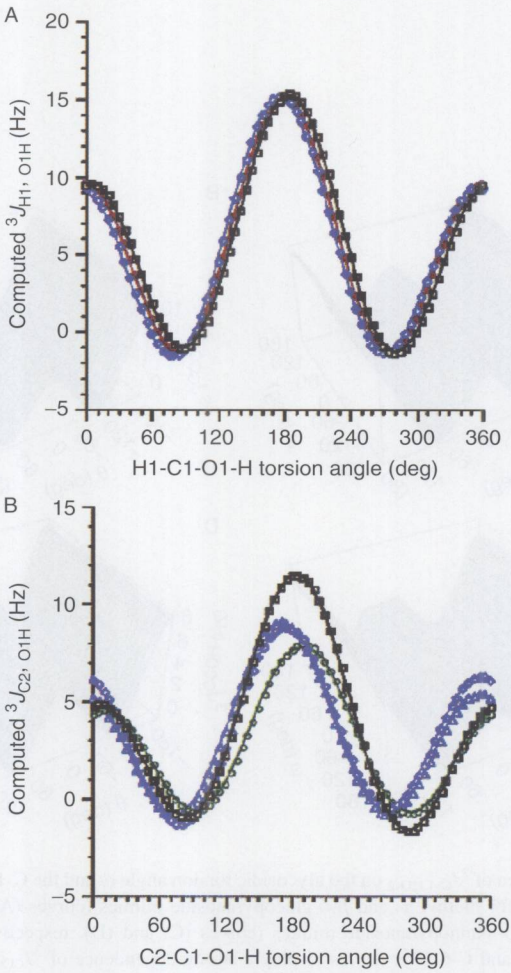

PLATE 1 (A) DFT calculated, four-quadrant plots of dependence of $^3J_{H\text{-}1,HO\text{-}1}$ on the torsion angle about C-1–O-1, for 3,4,6-trideoxy mimics of α-D-glucopyranose and α-D-mannopyranose (Eq. (32), blue triangles) and β-D-glucopyranose and β-D-mannopyranose (Eq. (33), black squares). The data are superimposed on a plot of Eq. (31), (red circles). (B) DFT dependence of $^3J_{C\text{-}2,HO\text{-}1}$ on the C-1–O-1 torsion angle in 3,4,6-trideoxy mimics of α-D-glucopyranose (Eq. (57), green circles), β-D-glucopyranose (Eq. (59), blue triangles), α-D-mannopyranose (Eq. (58), black squares), and β-D-mannopyranose (Eq. (60), purple diamonds). (See Fig. 3 in Chapter 3, p. 35.)

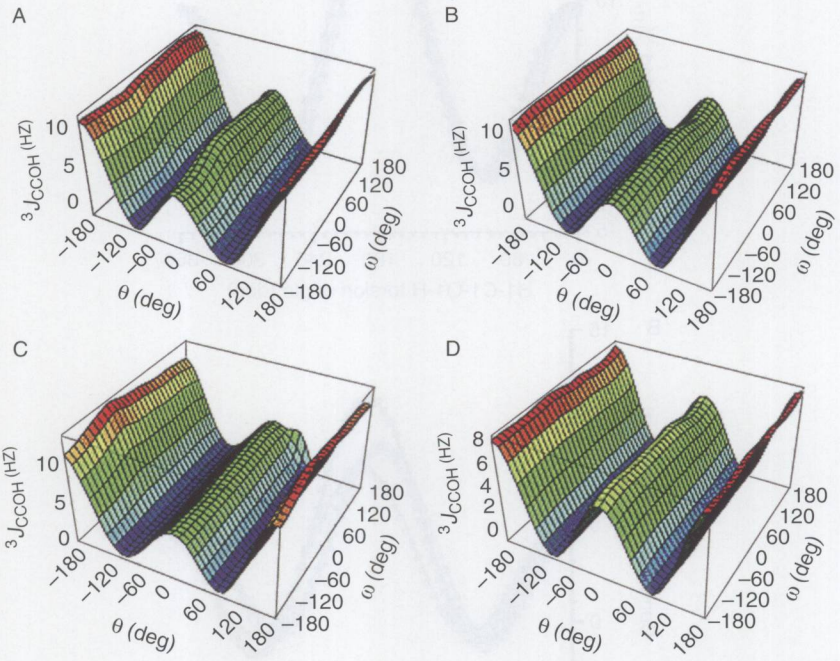

PLATE 2 Dependence of $^3J_{C\text{-}1,HO\text{-}2}$ on the glycosidic torsion angle ω and the C-1/HO-2 dihedral angle θ, as calculated by DFT for methyl α- and β-D-glucopyranoside mimics (curves (A) and (B), respectively) and methyl α- and β-D-mannopyranoside mimics (curves (C) and (D), respectively), all having deoxy functions at C-3, C-4, and C-6. The curves display a strong dependence of $^3J_{CCOH}$ on θ, and a minimal dependency on ω. (See Fig. 5 in Chapter 3, p. 44.)

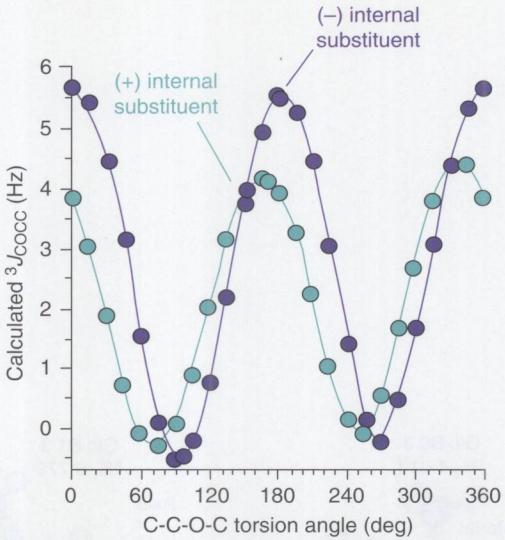

PLATE 3 Four-quadrant plots of DFT results for an ethyl β-D-glucopyranoside mimic of a disaccharide, showing phase shifting of $^3J_{CCOC}$ Karplus curves for C–C–O–C coupling pathways bearing an internal electronegative substituent. The mimic has deoxy functions at C-3, C-4, and C-6. (See Fig. 9 in Chapter 3, p. 56.)

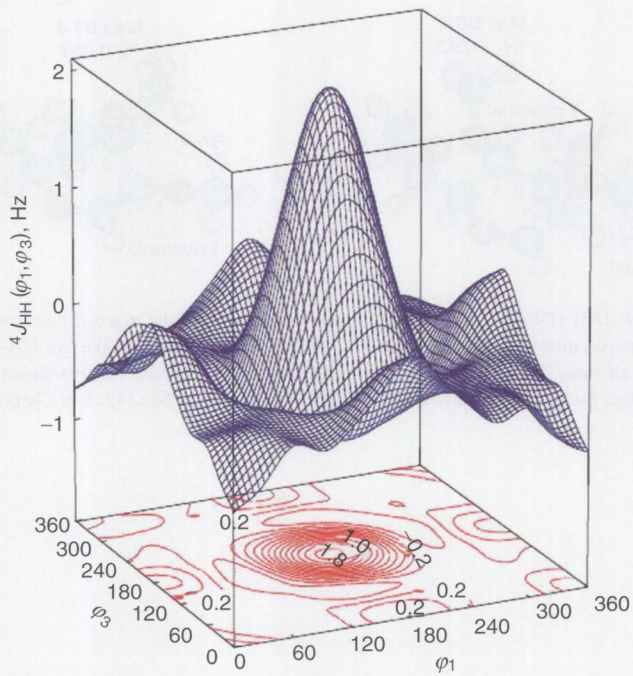

PLATE 4 3D plot and contour map for $^4J_{HCCCH}$ in propane, calculated as a function of the dihedral angles φ_1 and φ_3 by DFT/FPT at 30° intervals of the angles. 3D spline interpolations were used to create the graphs, which illustrate how the coupling constant changes sign, depending on the values of φ_1 and φ_3. A maximum positive value is seen for $\varphi_1 = \varphi_3 = 180°$. (See Fig. 10 in Chapter 3, p. 66.)

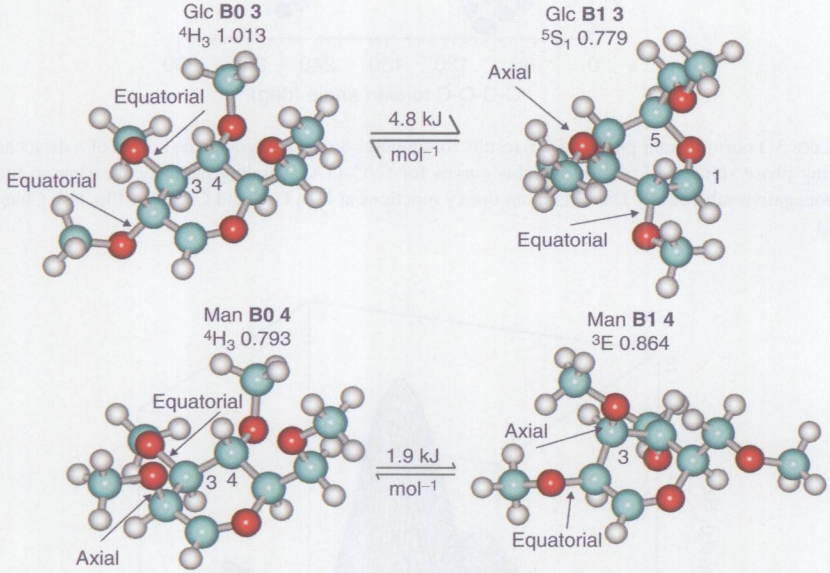

Plate 5 ADF–DFT (DPZ-frozen core)-optimized conformers of the *gluco* (**3**) and *manno* (**4**) isomers of **2**. Note the quasi-equatorial orientation of C-2–O-2 in all but **4 B0** and the *syn* CH-2-C-2–O-2C(H_3) conformation in all cases. The canonical vector with the highest coefficients is also shown. A coefficient of 1.0 equals a perfect match to that particular idealized conformation. (See Fig. 1 in Chapter 4, p. 91.)

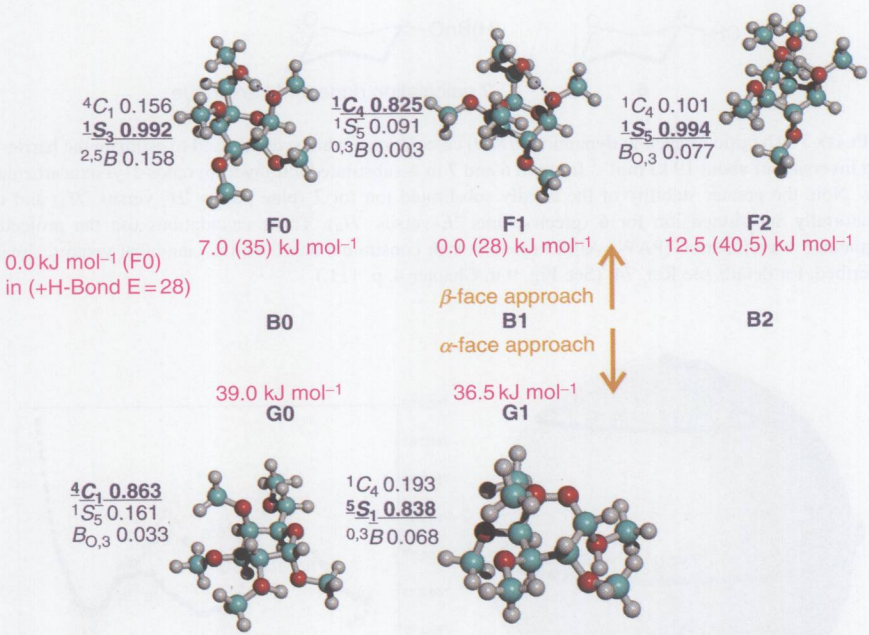

PLATE 6 Ball-and-stick representation of **2 F0, F1, F2**, and **G0** and **G1**. The top structures correspond to β-attack and the bottom structures to α-attack. The relative energies are also shown, with the values corrected for H-bonding shown in parentheses. (See Fig. 6 in Chapter 4, p. 103.)

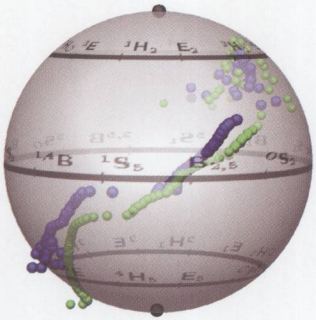

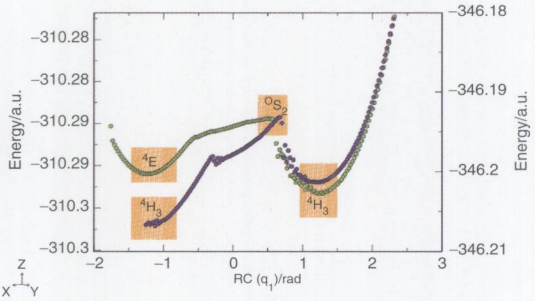

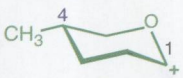

6

7 calculation done for H analogue

Plate 7 Ab initio molecular dynamic (AIMD) calculations, which can be used to estimate the barrier to ring inversion of about 19 kJ mol^{-1} for both **6** and **7** in 4-substituted tetrahydropyranos-1-yl oxacarbenium ions. Note the greater stability of the axially substituted ion for **7** (blue points $^4H_3$ versus $^3H_4$) and the equatorially substituted ion for **6** (green points ^4E versus $^3H_4$). These calculations use the projector-augmented wavefunction (PAW) AIMD method with constraints based on the canonical vectors already described, for details see Ref. 74. (See Fig. 9 in Chapter 4, p. 111.)

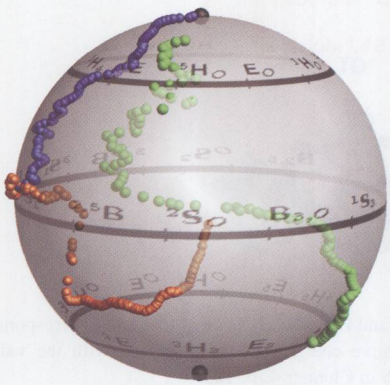

Green from $^4H_3$ **B0** conformation using q1 chair constraint, blue from $^5S_1$ **B1** conformation using q1 chair constraint and orange from $^2S_0$ using the q2 Boat constraint.

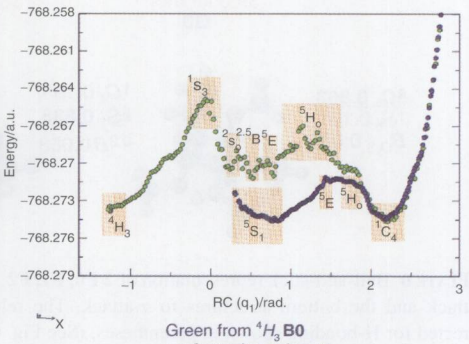

Green from $^4H_3$ **B0** conformation using q1 chair constraint and blue from $^5S_1$ **B1** conformation using q1 chair constraint.

Plate 8 AIMD trajectories of **3**. Left side: representative points plotted in 3D, and right side, corresponding absolute energies in a.u. The colors on the left and right are for the same trajectories. The $^1C_4$ minima in the right-hand side are for the 1,6-anhydro species as described above, for details see Ref. 74. (See Fig. 11 in Chapter 4, p. 113.)

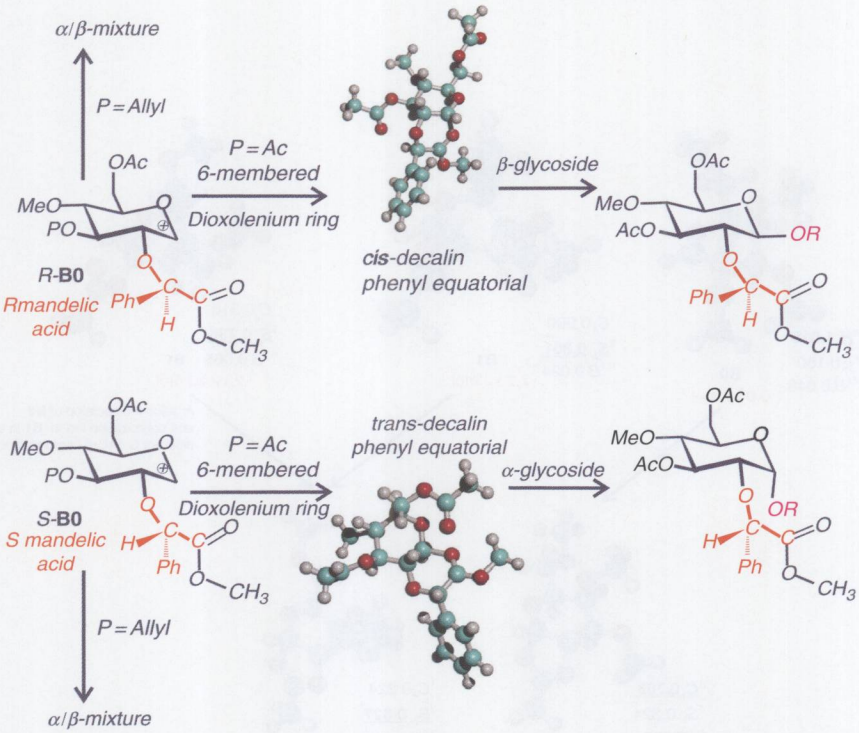

Plate 9 The *R*-mandelic acid (in gold)-based chiral auxiliary at O-2 can form a more-stable 6-membered dioxolenium ion, *trans*-decalin-like (32.9 kJ mol^{-1} relative to its **B0**), whereas its epimer can lead to a *cis*-decalin type of dioxolenium ion (72.8 kJ mol^{-1}), ADF–DFT (DPZ frozen core). The *trans*-decalin leads to α glycosides, whereas the *cis*-decalin leads to β glycosides. Both 6-membered-ring dioxolenium ions are more stable then any dioxolenium ion based on participation from O-3 (*R* 43.9 kJ mol^{-1} and *S* 46.7 kJ mol^{-1}). If R = allyl, then it is hypothesized that non-facially selective glycosylation takes place through the oxacarbenium ion (**B0** or **B1**). Note that the experiment used *O*-benzyl and not the *O*-methyl, which was used for the calculation to avoid complications of multiple minima. (See Fig. 12 in Chapter 4, p. 115.)

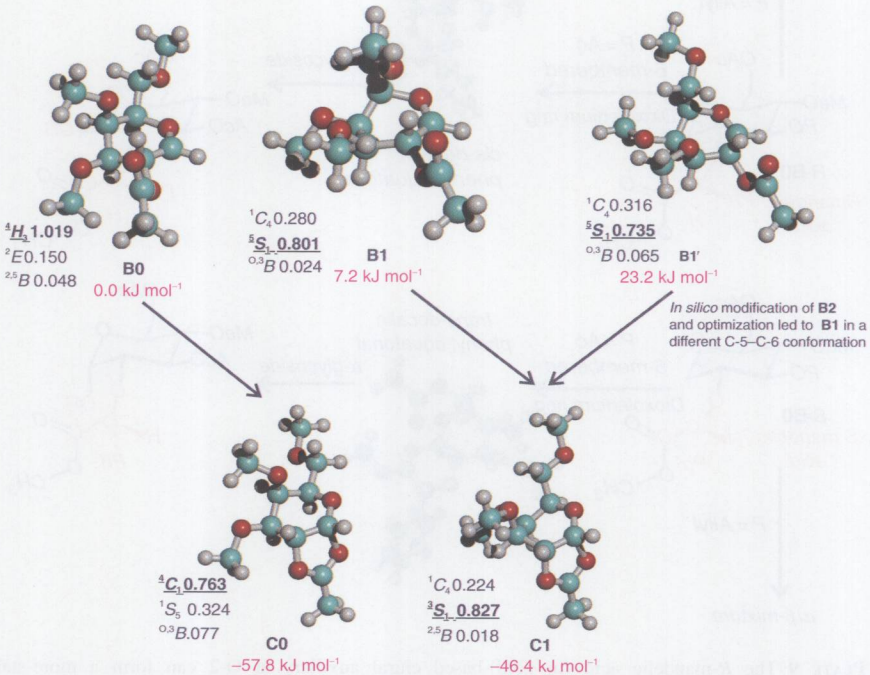

Plate 10 The ADF–DFT (TPZ) optimized **B0, B1**, and **B2** conformations of **17** and the related ring-closed dioxolenium ions **C0** and **C1**. The canonical-vector coefficients are also shown as well as the relative energies. (See Fig. 15 in Chapter 4, p. 122.)

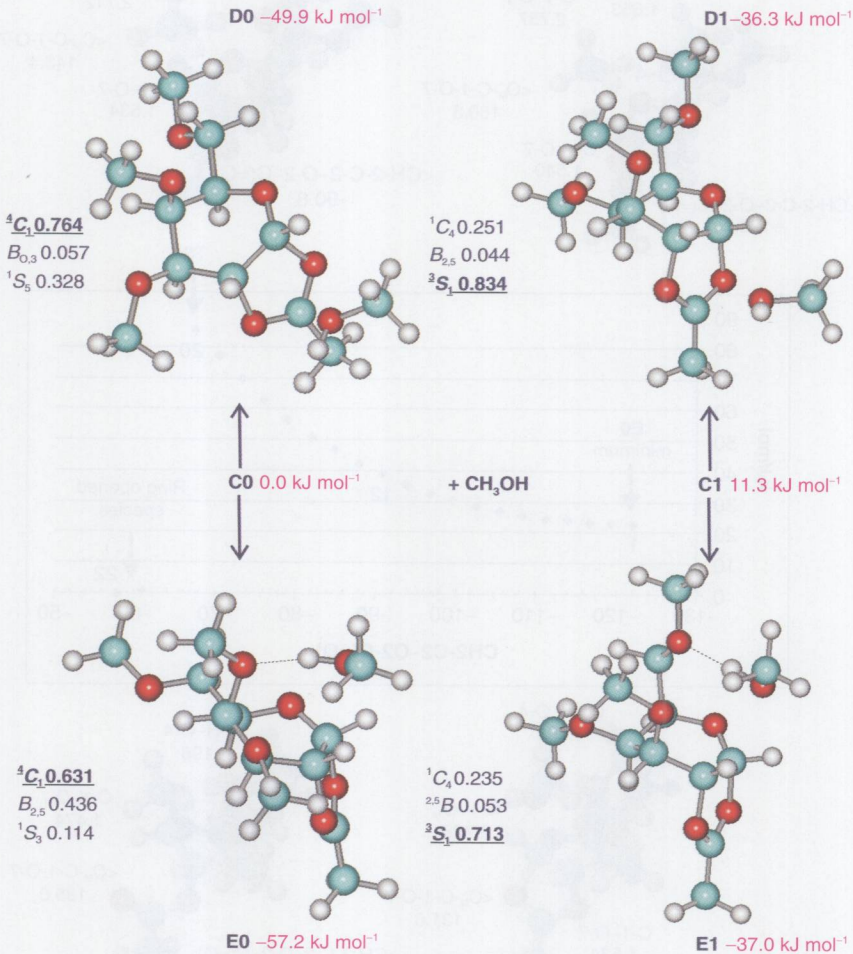

Plate 11 Ball and stick representation of the **D0, D1, E0**, and **E1** methanol complexes of **17**. (See Fig. 17 in Chapter 4, p. 127.)